Chloride, Bromide and Iodide Photo-Oxidation in Acetonitrile/Water Mixtures Using Binuclear Ir(III) Photosensitizers

Simon De Kreijger, ‡ Benjamin Elias‡ and Ludovic Troian-Gautier‡*

‡ UCLouvain, Institut de la Matière Condensée et des Nanosciences (IMCN), Molecular Chemistry, Materials and Catalysis (MOST), Place Louis Pasteur 1 box L4.01.02, B-1348 Louvain-la-Neuve, Belgium.

KEYWORDS. Halide photo-oxidation • Electron Transfer • Quenching • Energy Conversion • Cage-Escape Yields.

ABSTRACT: Two Ir(III) binuclear photosensitizers, $[Ir(dFCF_3ppy)_2(N–N)Ir(dFCF_3ppy)_2]^{2+}$, where N–N is tetrapyrido[3,2-a:2',3'-c:3",2"-h:2"',3"'-j]phenazine (Ir-TPPHZ) and 1,4,5,8-tetraazaphenanthrene[9,10-b]1,4,5,8,9,12-hexaazatriphenylene (Ir-TAPHAT) are reported for iodide, bromide and chloride photo-oxidation in acetonitrile and acetonitrile/water mixtures using blue light irradiation. Excited-state reduction potentials E_{red}^* of + 2.02 and + 2.09 V vs NHE were determined for Ir-TPPHZ and Ir-TAPHAT, respectively. Both photosensitizers' excited-states were efficiently quenched by iodide, bromide and chloride with quenching rate constants in the (3.5-9.2) $x10^{10}$ $M^{-1}s^{-1}$ and (0.0036-2.9) $x10^{10}$ $M^{-1}s^{-1}$ range in neat acetonitrile and acetonitrile/water mixtures, respectively. Nanosecond transient absorption spectroscopy provided unambiguous evidence of reductive excited-state electron transfer with all halides in solvent mixtures containing up to 50% of water. Cage-escape yields were large (96-55%) in acetonitrile and dropped below 32% in acetonitrile/water 50/50 mixtures.

Society is facing an energy crisis and novel approaches towards solar energy conversion are in dire need.[1-8] Different innovative technologies have been explored for the conversion of sunlight into useful energy sources. The storage of solar energy in chemical bonds of small molecules, so-called *solar fuels*, represents a highly promising avenue.[9-18] Among them, hydrogen gas (H_2) represents a promising target for large scale energy storage and distribution.[19] Hydrohalic acid (HX) splitting is the thermodynamically uphill conversion of HX to yield H_2 and the corresponding halogen (X_2). The reverse reaction releases free energy. Thus, rather than converting light directly into electrical power, solar photons can be stored in chemical bonds through HX splitting.[20]

HX splitting and water splitting are routes of great interest for solar hydrogen production. However, despite the considerable supply of water, the oxidation of H_2O to O_2 is a four-electron process that involves multiple proton-coupled electron transfer steps.[21] HX splitting is a mechanistically simpler alternative, as halides (X^-) are oxidized to X_2 by a two-electron transfer process that does not involve proton-coupled electron transfer steps.[15]

Aqueous halide oxidation occurs at potentials $E_{1/2}(X^{\bullet/-})$ of 1.33, 1.93 and ~2.1-2.3V vs NHE for iodide, bromide and chloride, respectively.[15] This renders bromide and chloride photo-oxidation extremely challenging to perform in water with visible light. This wide range of potentials was shown to be narrower in organic solvents. For example, $E_{1/2}(X^{\bullet/-})$ of 1.23, 1.35 and 1.46 V vs NHE have been roughly estimated in acetonitrile for iodide, bromide and chloride, respectively.[22-23] These potentials were estimated via Marcus theory using experimentally determined kinetic quenching rate constants. Experimental evidence for photo-induced electron transfer from bromide and iodide to photo-excited Ru and Ir photosensitizers was demonstrated in acetonitrile by transient absorption spectroscopy, but corresponding experimental evidence for chloride oxidation is still missing. [22-23] This is presumably due to the very fast back electron transfer between the oxidized halide and reduced photosensitizer. Strategies to prevent this fast back-electron transfer using secondary coordination effects were proposed by Nocera *et al.* and used aryl substituents to form Cl˙|arene adducts that could be experimentally observed.[24-27] Notably bromide and chloride photo-oxidation have been monitored in acetone using Ru(II) photosensitizers[28-30] as well as by one- or two-photon excitation of N-phenylphenothiazine in acetonitrile.[31]

Here, we focused on novel Ir(III) photosensitizers with very high photo-oxidizing abilities that, upon visible light irradiation, reacted with halides in acetonitrile/water mixtures. Cyclometalated iridium(III) photosensitizers are an outstanding class of compounds, possessing spatially separated frontier orbitals, meaning that the C–N centered HOMO and N–N centered LUMO levels can be independently tuned, leading to ease of changes in excited-state reduction potentials.[32] Hence, two binuclear Ir(III) photosensitizers bearing the **dFCF$_3$ppy** (2-(2,4-difluorophenyl)-5-(trifluoromethyl)pyridine) ancillary ligand and in combination with the π-extended diimine ligand **TPPHZ** (tetrapyrido[3,2-a:2',3'-c:3",2"-h:2"',3"'-j]phenazine) and **TAPHAT** (1,4,5,8-tetraazaphenanthrene[9,10-b]1,4,5,8,9,12-hexaazatriphenylene) were designed (**Figure 1**). They exhibited excellent excited-state reactivity toward iodide, bromide and chloride, as emphasized by the drastic quenching of the steady-state and time-resolved photoluminescence, with quenching rate constants (k_q) up to 10^{10} $M^{-1}s^{-1}$. Further investigation by transient absorption spectroscopy proved efficient electron transfer from iodide, bromide and chloride to the excited photosensitizers even in acetonitrile/water mixtures.

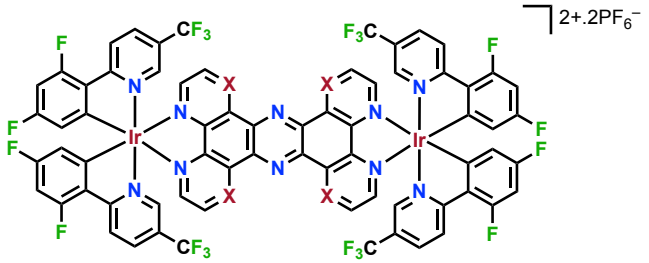

X = CH, $[Ir(dFCF_3ppy)_2(TPPHZ)Ir(dFCF_3ppy)_2]^{2+}.2PF_6^-$ (**Ir-TPPHZ**)
X = N, $[Ir(dFCF_3ppy)_2(TAPHAT)Ir(dFCF_3ppy)_2]^{2+}.2PF_6^-$ (**Ir-TAPHAT**)

Figure 1. Structures of Ir-TPPHZ (X = CH) and Ir-TAPHAT (X = N).

Both photosensitizers were obtained via the reaction between $[Ir(dFCF_3ppy)_2(\mu\text{-}Cl)]_2$ and the corresponding TPPHZ or TAPHAT ligand, which were synthesized using literature procedures.[33-34] This yielded $[Ir(dFCF_3ppy)_2(TPPHZ)Ir(dFCF_3ppy)_2]^{2+}$ (Ir-TPPHZ) and $[Ir(dFCF_3ppy)_2(TAPHAT)Ir(dFCF_3ppy)_2]^{2+}$ (Ir-TAPHAT) in 70% and 68% yield, respectively. Both photosensitizers were characterized by UV-Visible absorption which showed typical ligand-centered (LC) transitions below 400 nm with mixed metal-ligand to ligand charge transfer (MLLCT) transitions in the visible (**Figure 2**). Both photosensitizers absorbed in the visible, Ir-TPPHZ at 420 nm (ε=6400 $M^{-1}cm^{-1}$) and Ir-TAPHAT at 450nm (ε=5200 $M^{-1}cm^{-1}$).

Steady-state photoluminescence measurements performed in acetonitrile displayed intense photoluminescence centered at 613 and 635 nm for Ir-TPPHZ and Ir-TAPHAT, respectively. Time-resolved photoluminescence was well described by single-exponential decay from which excited-state lifetimes were determined for Ir-TPPHZ (618 ns) and Ir-TAPHAT (152 ns). These photophysical, as well as ground and excited-state electrochemical properties are gathered in **Table 1**.

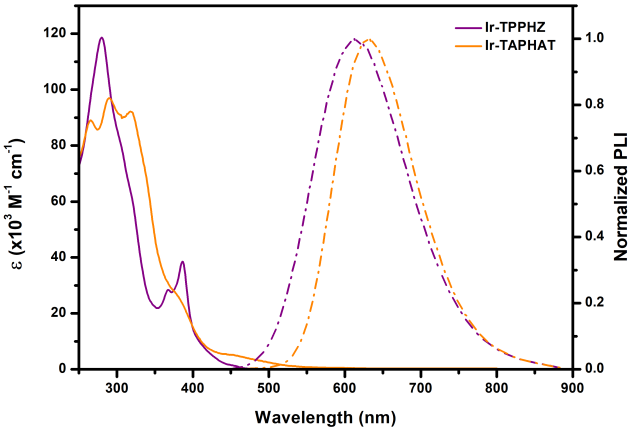

Figure 2. UV-Visible absorption (solid) and steady-state photoluminescence (dashed) spectra of Ir-TPPHZ (purple) and Ir-TAPHAT (orange) recorded in argon-purged acetonitrile at room temperature.

Table 1. Photophysical and ground- and excited-state electrochemical properties of Ir-TPPHZ and Ir-TAPHAT.

	λ_{Abs} (nm), [ε,$10^3 M^{-1}cm^{-1}$][a]	PL_{max} (nm)[a]	τ (ns)[a]	τ (ns)[b]	τ (ns)[c]	E_{ox}[d]	E_{red}[d]	E_{ox}*[d]	E_{red}*[d]
Ir-TPPHZ	386 (38.5), 420 (6.4)	613	618	215	125	2.03	– 0.45	– 0.45	2.02
Ir-TAPHAT	385 (23.8), 450 (5.2)	635	152	19	17	2.14	– 0.21	– 0.15	2.09

[a] In argon-purged acetonitrile. [b] In argon-purged acetonitrile/Water 75:25. [c] In argon-purged acetonitrile/Water 50:50. [d] V vs NHE.

Table 2. Quenching rate constants for Ir-TPPHZ and Ir-TAPHAT with I^-, Br^- and Cl^- in acetonitrile/water mixtures

	k_q ($M^{-1}s^{-1}$) with Ir-TPPHZ			k_q ($M^{-1}s^{-1}$) with Ir-TAPHAT		
	CH_3CN	$CH_3CN:H_2O$ 75:25	$CH_3CN:H_2O$ 50:50	CH_3CN	$CH_3CN:H_2O$ 75:25	$CH_3CN:H_2O$ 50:50
Iodide	9.2×10^{10}	2.9×10^{10}	2.1×10^{10}	6.8×10^{10}	2.6×10^{10}	2.0×10^{10}
Bromide	6.2×10^{10}	9.5×10^{9}	4.3×10^{9}	4.4×10^{10}	8.9×10^{9}	4.8×10^{9}
Chloride	5.1×10^{10}	4.5×10^{7}	3.6×10^{7}	3.5×10^{10}	2.0×10^{8}	1.3×10^{8}

Excited-state quenching of both sensitizers with iodide, bromide and chloride was carried out in acetonitrile under argon atmosphere. Stern-Volmer experiments revealed that all halides were competent for dynamic excited-state quenching (**Figure 3**) with quenching rate constants (k_q) that ranged from 3.5×10^{10} to 9.2×10^{10} $M^{-1}s^{-1}$ (**Table 2**).

As Stern-Volmer experiments do not inform on the nature of the excited-state quenching process, nanosecond transient absorption spectroscopy (nsTAS) was used. Ir-TPPHZ and Ir-TAPHAT were individually irradiated using pulsed 410 nm light irradiation in the presence of iodide, bromide or chloride in argon purged acetonitrile (**Figure 4**). The appearance of a long-lived transient species absorbing around 600 nm was consistent with the formation of mono-reduced photosensitizers by electron transfer from iodide, as confirmed by control experiments with tri-*p*-tolylamine, a known electron donor (**Figure S23**). Remarkably, the absorption changes were also observed in the presence of bromide or chloride, albeit with lower intensity. This is a striking result, as experimental substantiation for chloride oxidation has been to date scarcely reported in the literature while here, we show unambiguous confirmation of photo-induced electron transfer from chloride to both Ir-TPPHZ and Ir-TAPHAT. Note that evidence for $I_2^{\bullet-}$ formation was obtained at higher concentrations of TBAI, with additional absorption features around 400 nm and 750 nm (**Figure S24**).[35, 36]

Motivated by these results and given the very positive excited-state reduction potential of Ir-TPPHZ and Ir-TAPHAT, we performed excited-state quenching experiments in

acetonitrile/water mixtures. Both photosensitizers were efficiently quenched by iodide and bromide in mixtures containing up to 50% water, with quenching rate constants in the ~10^{10} $M^{-1}s^{-1}$ and 10^9 $M^{-1}s^{-1}$ range for iodide and bromide, respectively. Excited-state quenching was also observed with chloride, albeit with a lower k_q (10^7-10^8 $M^{-1}s^{-1}$), as expected from thermodynamic parameters (**Figure 3**). Yet, the observed excited-state quenching was very encouraging, and nsTAS experiments were carried out with both photosensitizers in acetonitrile/water 50/50 mixture (**Figure 4 c-d**).[37] Formation of the monoreduced Ir-TPPHZ and Ir-TAPHAT was observed by nsTAS, demonstrating that halide oxidation occurred efficiently in water-enriched conditions. With Ir-TAPHAT, using chloride or bromide, an additional band around 500 nm was observed. At this stage, we were unable to unambiguously ascribe this novel absorption band, but we hypothesize that it could originate from an intramolecular X•|arene adduct with the TAPHAT ligand.[38] Nevertheless, the transition around 600 nm point towards excited-state halide oxidation in acetonitrile/water 50/50 mixture. Importantly, at this solvent ratio, the steady-state UV absorption spectrum of iodide closely resembles the one obtained in neat water (**Figure 5**), suggesting a similar solvation of the halide as in neat water. Similar experiments on chloride and bromide were limited due to the lack of absorption above 200 nm. It is therefore likely that the one-electron reduction potential of each halide in acetonitrile/water 50/50 mixture is close to the one determined in neat water.

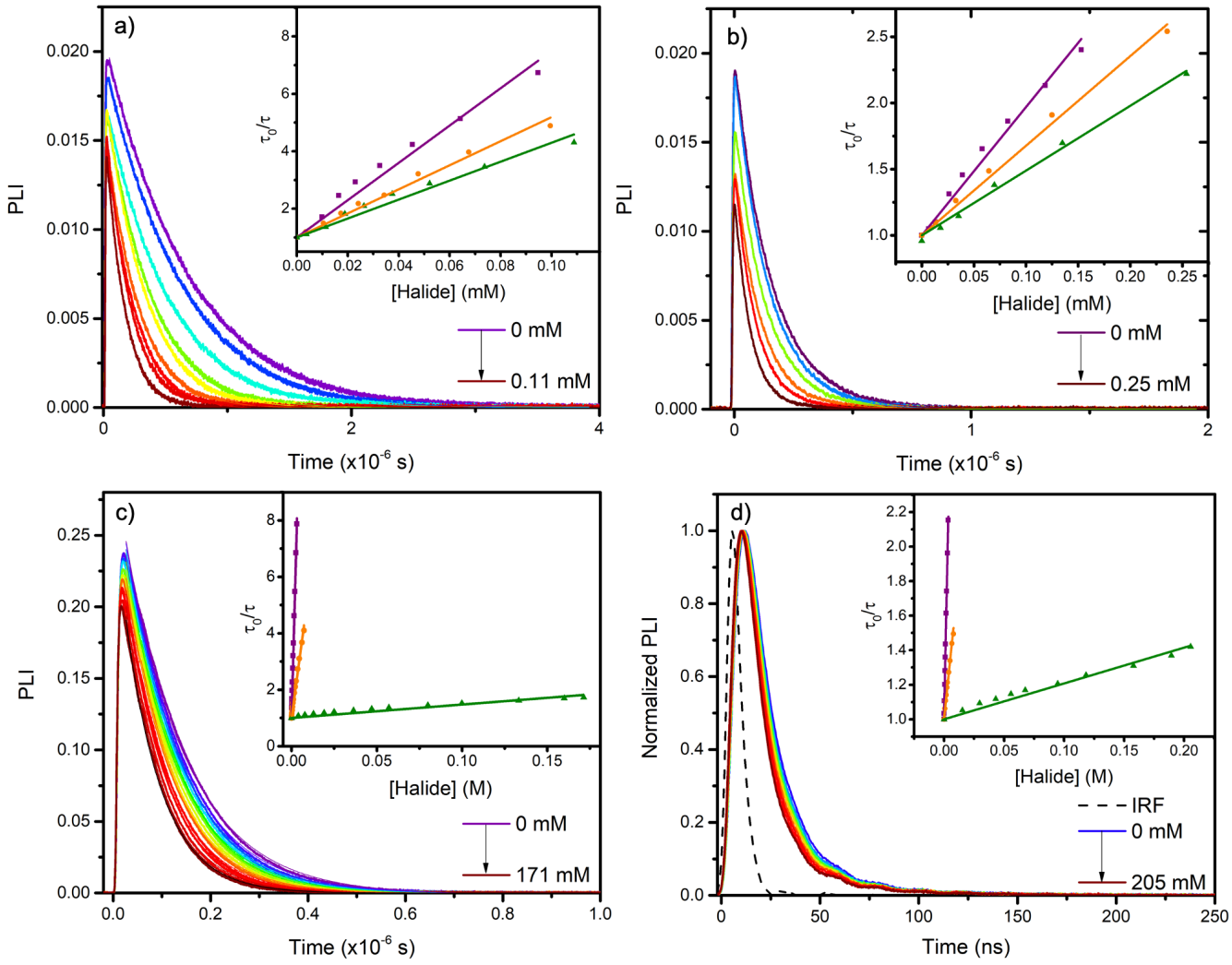

Figure 3. Time-resolved photoluminescence of Ir-TPPHZ (a,c) and Ir-TAPHAT (b,d) with increasing amount of tetrabutylammonium chloride in acetonitrile (a,b) and acetonitrile/water 50/50 (c,d). The inset shows the corresponding Stern-Volmer plots obtained with iodide (purple), bromide (orange) and chloride (green). The corresponding quenching rate constants are gathered in **Table 2**.

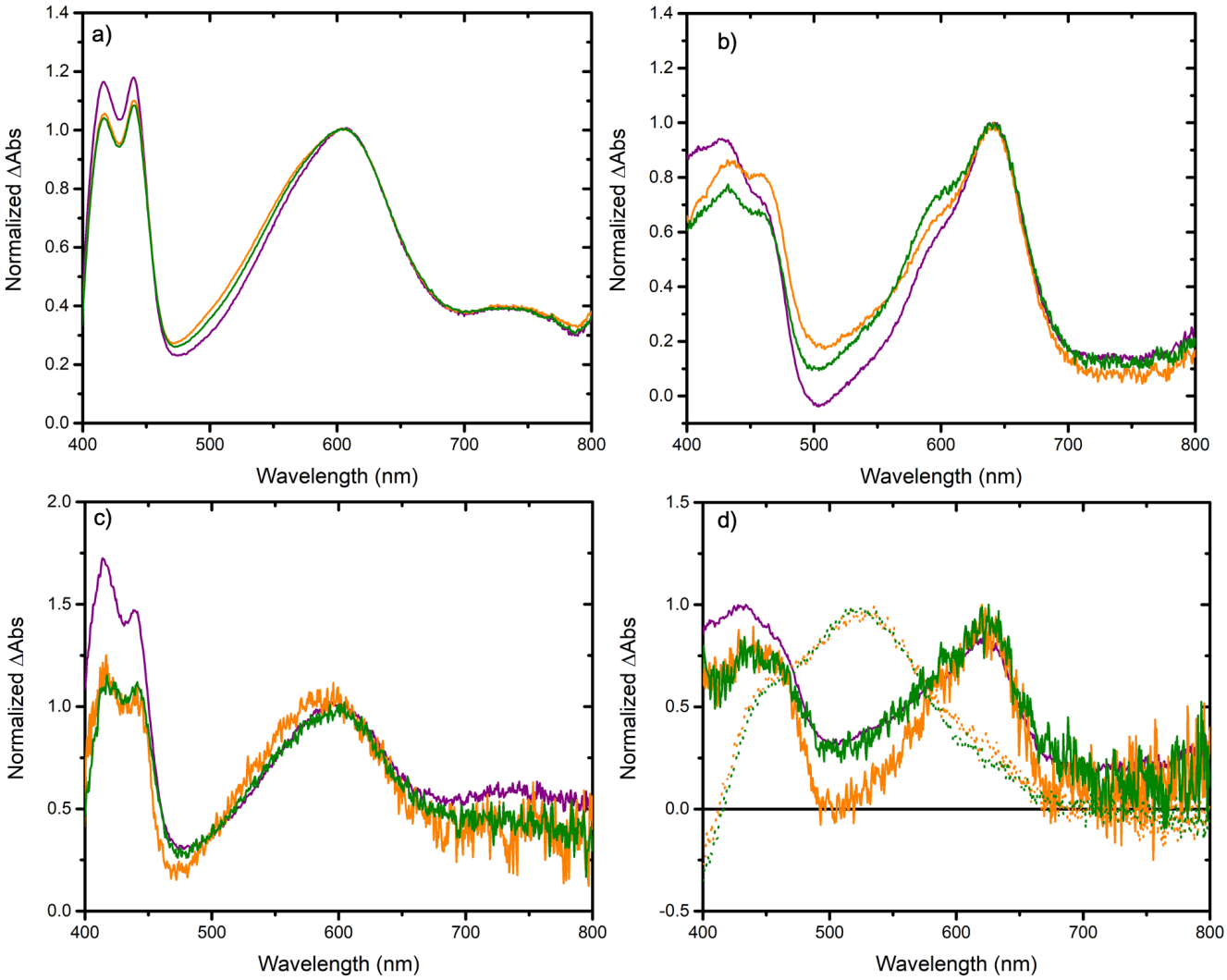

Figure 4. Transient absorption spectra of Ir-TPPHZ (a) and Ir-TAPHAT (b) recorded with 1 mM iodide (purple), 1 mM bromide (orange) and 1 mM chloride (green) in acetonitrile (a,b). Transient absorption spectra of Ir-TPPHZ (c) and Ir-TAPHAT (d) recorded in acetonitrile/water 50/50 mixture in the presence of 10 mM iodide (purple), 10 mM bromide (orange (dots: 500ns; solid: 30 µs after the laser pulse)) or 200 mM chloride (green (dots: 500ns; solid: 30 µs after the laser pulse)). Experiments were carried out in argon-purged solution at room temperature using 410 nm light irradiation. Spectra were recorded 500 ns after the laser pulse, unless otherwise specified. Non-normalized spectra are shown in Figures S11-S22.

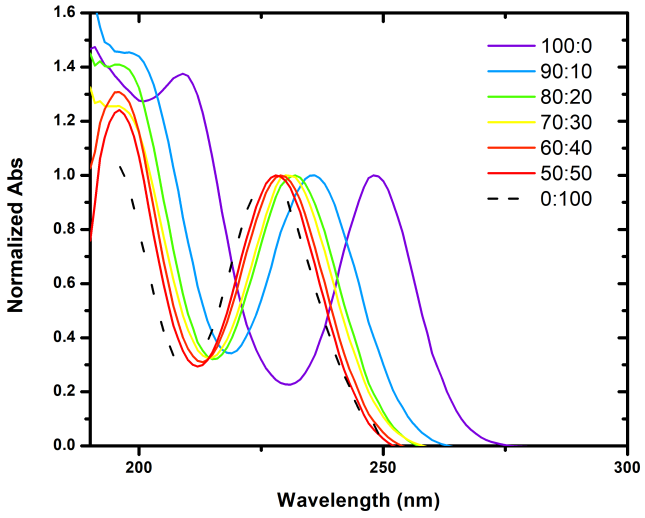

Figure 5. UV absorption spectra of *tetra-n*-butyliodide recorded in acetonitrile/water 100/0 → 50/50 mixtures (solid lines) compared to the one of potassium iodide (dashed black line) in water.

Finally, cage-escape yields, *i.e.* the efficiency with which the geminate radical pair (i.e. the monoreduced binuclear iridium photosensitizer and oxidized halide) separate after excited-state electron transfer was quantified using nsTAS.[39] Quantifying this process is of interest as it was shown to impact the subsequent reactions that can be performed using these solvent-separated radicals.[39-42] Here, cage-escape yields were determined by comparative actinometry using Eq. 1 and 2 with $[Ru(bpy)_3]^{2+}$ as actinometer.[43]

$$\Phi_{CE} = \frac{\Phi}{\%\ PL\ Quenched} \qquad \text{Eq. 1}$$

$$\Phi = \left(\frac{\frac{\Delta A_{PS^-}}{\Delta \varepsilon_{PS^-}}}{\frac{\Delta A_{ES_{ref}}}{\Delta \varepsilon_{ES_{ref}}}} \right) \left(\frac{1-10^{-Abs_{ref}(\lambda exc)}}{1-10^{-Abs_{PS}(\lambda exc)}} \right) \qquad \text{Eq. 2}$$

The transient absorption changes at 600 nm or 620 nm corresponding to the singly reduced Ir-TPPHZ and Ir-TAPHAT, respectively, were compared to the changes in absorption of the reference $[Ru(bpy)_3]^{2+}$ (ES_{ref}) at 450nm. A $\Delta\varepsilon$ value of –10100 $M^{-1}cm^{-1}$ was used for the actinometer at 450 nm[44-46] while $\Delta\varepsilon_{620nm}$ = 6500 $M^{-1}cm^{-1}$ and $\Delta\varepsilon_{600nm}$ = 9500 $M^{-1}cm^{-1}$ were determined by nsTAS using tri-*p*-tolylamine for Ir-TAPHAT and Ir-TPPHZ, respectively (**Figure S23**). Cage-escape yields (ϕ_{CE}) values were obtained by comparing the relative yield of mono-reduced PS produced (ϕ) to the percentage of quenched PL (%PL) (**Figure 6**).

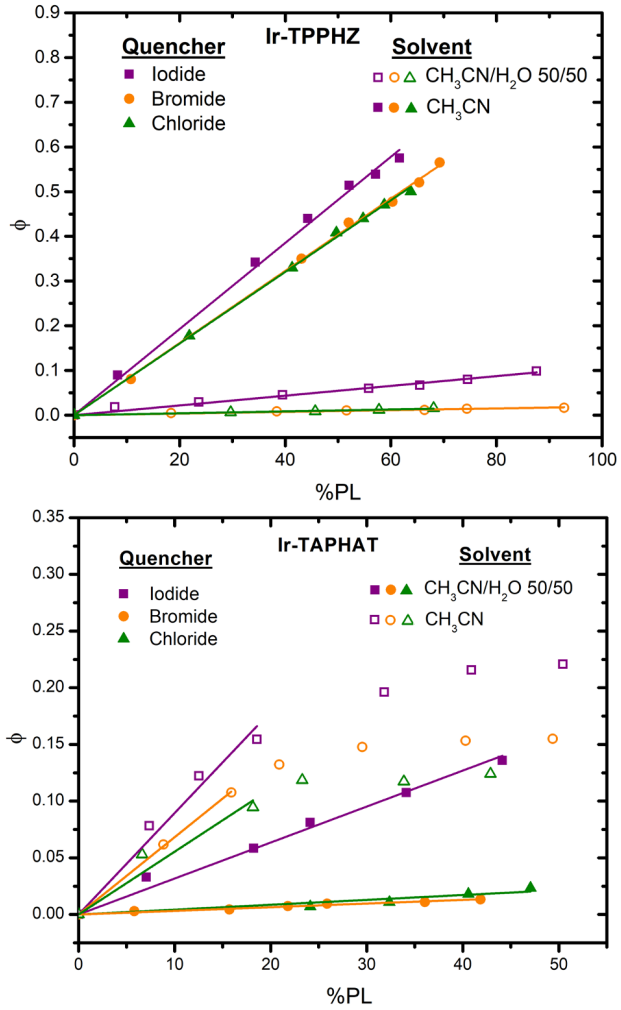

Figure 6. Cage-escape yields recorded using Ir-TPPHZ (top) and Ir-TAPHAT (bottom) in argon-purged CH_3CN (open symbols) and CH_3CN/H_2O 50/50 (closed symbols) in the presence of iodide (purple), bromide (orange) and chloride (green).

Table 3. Cage-escape yields (Φ_{CE}) recorded in argon-purged CH_3CN and CH_3CN/H_2O

	Φ_{CE} Ir-TAPHAT		Φ_{CE} Ir-TPPHZ	
	CH_3CN	CH_3CN/H_2O	CH_3CN	CH_3CN/H_2O
I^-	90%	32%	96%	11%
Br^-	70%	3%	81%	2%
Cl^-	55%	4%	80%	2%

Whether in acetonitrile or acetonitrile/water 50/50, ϕ_{CE} followed the periodic trend I>Br>Cl (**Table 3**). In acetonitrile/water 50/50, ϕ_{CE} were slightly larger for Ir-TAPHAT than for Ir-TPPHZ. This difference was most prominent with iodide where ϕ_{CE} were three times larger for Ir-TAPHAT than for Ir-TPPHZ. In acetonitrile, the picture is slightly different. For Ir-TPPHZ, the experimental data evolved linearly with concentration and ϕ_{CE} were calculated from the entire slope. This yielded ϕ_{CE} values that ranged from 91% to 80% for iodide and chloride, respectively. For Ir-TAPHAT, the data was only linear until approximately one equivalent of halide was added. From that initial slope, cage-escape yields between 90% and 55% were determined. It should be noted that literature reports of ϕ_{CE} often rely on single concentration measurements, while those provided herein yield a broader description of the cage-escape process. The change of slope around 1 equivalent of added halide probably points toward an ion-paired quenching mechanism[47-50] and highlight that this cage-escape process could evolve over a range of concentration. This will be investigated in the future.

In conclusion, we report two novel binuclear Ir(III) photosensitizers that were shown to be efficiently quenched by iodide, bromide and chloride in neat acetonitrile and acetonitrile/water mixtures. Importantly, nsTAS revealed that excited-state electron transfer of all investigated halides occurred efficiently with large to moderate cage-escape yields. Noteworthy, this experimental verification of excited-state electron transfer also held true in acetonitrile/water mixtures, containing up to 50% of water, further expanding the applicability of these type of photosensitizers as candidates for hydrohalic acid splitting. Overall, the ϕ_{CE} measurement also indicated that small structural changes, such as the introduction of two nitrogen atom in the bridging ligand scaffold, have a drastic impact on the charged species separation processes.

AUTHOR INFORMATION

Corresponding Author

*Ludovic.Troian@uclouvain.be

Author Contributions

The manuscript was written through contributions of all authors. All authors have given approval to the final version of the manuscript.

Funding Sources

Grant no. U.N021.21 (B.E.).

ASSOCIATED CONTENT

Supporting Information: Experimental details, synthesis of novel compounds, ^{1}H NMR spectra and HR-MS for all new compounds, Stern-Volmer experiments, transient absorption spectroscopy (pdf). The Supporting Information is available free of charge on the ACS Publications website.

ACKNOWLEDGMENT

This work was supported by the Fonds de la Recherche Scientifique (F.R.S.-FNRS) under grant no. U.N021.21 (B.E.). L.T.-G. is a Chercheur Qualifié of the Fonds de la Recherche Scientifique – FNRS. S.D.K., B.E. and L.T.-G. gratefully acknowledge the UCLouvain for financial support.

ABBREVIATIONS

TAPHAT: 1,4,5,8-tetraazaphenanthrene[9,10-b]1,4,5,8,9,12-hexaazatriphenylene
TPPHZ: tetrapyrido[3,2-a:2',3'-c:3",2"-h:2"',3"'-j]phenazine
dFCF$_3$ppy: (2-(2,4-difluorophenyl)-5-(trifluoromethyl)pyridine)

REFERENCES

1. Nocera, D. G., Chemistry of Personalized Solar Energy. *Inorg. Chem.* **2009,** *48*, 10001-10017.
2. Nocera, D. G., The Artificial Leaf. *Acc. Chem. Res.* **2012,** *45*, 767-776.
3. Brennaman, M. K.; Dillon, R. J.; Alibabaei, L.; Gish, M. K.; Dares, C. J.; Ashford, D. L.; House, R. L.; Meyer, G. J.; Papanikolas, J. M.; Meyer, T. J., Finding the Way to Solar Fuels with Dye-Sensitized Photoelectrosynthesis Cells. *J. Am. Chem. Soc.* **2016,** *138*, 13085-13102.
4. Andreiadis, E. S.; Chavarot-Kerlidou, M.; Fontecave, M.; Artero, V., Artificial Photosynthesis: From Molecular Catalysts for Light-driven Water Splitting to Photoelectrochemical Cells. *Photochem. Photobiol.* **2011,** *87*, 946-964.
5. Windle, C. D.; Kumagai, H.; Higashi, M.; Brisse, R.; Bold, S.; Jousselme, B.; Chavarot-Kerlidou, M.; Maeda, K.; Abe, R.; Ishitani, O.; Artero, V., Earth-Abundant Molecular Z-Scheme Photoelectrochemical Cell for Overall Water-Splitting. *J. Am. Chem. Soc.* **2019,** *141*, 9593-9602.
6. Kar, S.; Rahaman, M.; Andrei, V.; Bhattacharjee, S.; Roy, S.; Reisner, E., Integrated capture and solar-driven utilization of CO₂ from flue gas and air. *Joule*.
7. Bhattacharjee, S.; Rahaman, M.; Andrei, V.; Miller, M.; Rodríguez-Jiménez, S.; Lam, E.; Pornrungroj, C.; Reisner, E., Photoelectrochemical CO2-to-fuel conversion with simultaneous plastic reforming. *Nature Synthesis* **2023,** *2*, 182-192.
8. Rahaman, M.; Andrei, V.; Wright, D.; Lam, E.; Pornrungroj, C.; Bhattacharjee, S.; Pichler, C. M.; Greer, H. F.; Baumberg, J. J.; Reisner, E., Solar-driven liquid multi-carbon fuel production using a standalone perovskite–BiVO4 artificial leaf. *Nat. Energy* **2023,** *8*, 629-638.
9. Wang, Q.; Pornrungroj, C.; Linley, S.; Reisner, E., Strategies to improve light utilization in solar fuel synthesis. *Nat. Energy* **2022,** *7*, 13-24.
10. Spitler, M. T.; Modestino, M. A.; Deutsch, T. G.; Xiang, C. X.; Durrant, J. R.; Esposito, D. V.; Haussener, S.; Maldonado, S.; Sharp, I. D.; Parkinson, B. A.; Ginley, D. S.; Houle, F. A.; Hannappel, T.; Neale, N. R.; Nocera, D. G.; McIntyre, P. C., Practical challenges in the development of photoelectrochemical solar fuels production. *Sustainable Energy Fuels* **2020,** *4*, 985-995.
11. Segev, G.; Kibsgaard, J.; Hahn, C.; Xu, Z. J.; Cheng, W.-H.; Deutsch, T. G.; Xiang, C.; Zhang, J. Z.; Hammarström, L.; Nocera, D. G.; Weber, A. Z.; Agbo, P.; Hisatomi, T.; Osterloh, F. E.; Domen, K.; Abdi, F. F.; Haussener, S.; Miller, D. J.; Ardo, S.; McIntyre, P. C.; Hannappel, T.; Hu, S.; Atwater, H.; Gregoire, J. M.; Ertem, M. Z.; Sharp, I. D.; Choi, K.-S.; Lee, J. S.; Ishitani, O.; Ager, J. W.; Prabhakar, R. R.; Bell, A. T.; Boettcher, S. W.; Vincent, K.; Takanabe, K.; Artero, V.; Napier, R.; Cuenya, B. R.; Koper, M. T. M.; Van De Krol, R.; Houle, F., The 2022 solar fuels roadmap. *Journal of Physics D: Applied Physics* **2022,** *55*, 323003.
12. Dogutan, D. K.; Nocera, D. G., Artificial Photosynthesis at Efficiencies Greatly Exceeding That of Natural Photosynthesis. *Acc. Chem. Res.* **2019,** *52*, 3143-3148.
13. Bold, S.; Massin, J.; Giannoudis, E.; Koepf, M.; Artero, V.; Dietzek, B.; Chavarot-Kerlidou, M., Spectroscopic Investigations Provide a Rationale for the Hydrogen-Evolving Activity of Dye-Sensitized Photocathodes Based on a Cobalt Tetraazamacrocyclic Catalyst. *ACS Catal.* **2021,** *11*, 3662-3678.
14. Sampaio, R. N.; Troian-Gautier, L.; Meyer, G. J., A Charge-Separated State that Lives for Almost a Second at a Conductive Metal Oxide Interface. *Angew. Chem.* **2018,** *130*, 15616-15620.
15. Troian-Gautier, L.; Turlington, M. D.; Wehlin, S. A. M.; Maurer, A. B.; Brady, M. D.; Swords, W. B.; Meyer, G. J., Halide Photoredox Chemistry. *Chemical Reviews* **2019,** *119*, 4628-4683.
16. Hu, K.; Sampaio, R. N.; Schneider, J.; Troian-Gautier, L.; Meyer, G. J., Perspectives on Dye Sensitization of Nanocrystalline Mesoporous Thin Films. *J. Am. Chem. Soc.* **2020,** *142*, 16099-16116.
17. De Kreijger, S.; Schott, O.; Troian-Gautier, L.; Cauët, E.; Hanan, G. S.; Elias, B., Red Absorbing Cyclometalated Ir(III) Diimine Photosensitizers Competent for Hydrogen Photocatalysis. *Inorg. Chem.* **2022,** *61*, 5245-5254.
18. Cotic, A.; Cerfontaine, S.; Slep, L. D.; Elias, B.; Troian-Gautier, L.; Cadranel, A., Anti-Dissipative Strategies toward More Efficient Solar Energy Conversion. *J. Am. Chem. Soc.* **2023,** *145*, 5163-5173.
19. Bolton, J. R., Solar photoproduction of hydrogen: A review. *Sol. Energy* **1996,** *57*, 37-50.
20. Brady, M. D.; Sampaio, R. N.; Wang, D.; Meyer, T. J.; Meyer, G. J., Dye-Sensitized Hydrobromic Acid Splitting for Hydrogen Solar Fuel Production. *Journal of the American Chemical Society* **2017,** *139*, 15612-15615.
21. Dau, H.; Limberg, C.; Reier, T.; Risch, M.; Roggan, S.; Strasser, P., The Mechanism of Water Oxidation: From Electrolysis via Homogeneous to Biological Catalysis. *ChemCatChem* **2010,** *2*, 724-761.
22. Bevernaegie, R.; Wehlin, S. A. M.; Piechota, E. J.; Abraham, M.; Philouze, C.; Meyer, G. J.; Elias, B.; Troian-Gautier, L., Improved Visible Light Absorption of Potent Iridium(III) Photo-oxidants for Excited-State Electron Transfer Chemistry. *J. Am. Chem. Soc.* **2020,** *142*, 2732-2737.
23. Deetz, A. M.; Troian-Gautier, L.; Wehlin, S. A. M.; Piechota, E. J.; Meyer, G. J., On the Determination of Halogen Atom Reduction Potentials with Photoredox Catalysts. *J. Phys. Chem. A* **2021,** *125*, 9355-9367.
24. Hwang, S. J.; Anderson, B. L.; Powers, D. C.; Maher, A. G.; Hadt, R. G.; Nocera, D. G., Halogen Photoelimination from Monomeric Nickel(III) Complexes Enabled by the Secondary Coordination Sphere. *Organometallics* **2015,** *34*, 4766-4774.
25. Hwang, S. J.; Powers, D. C.; Maher, A. G.; Anderson, B. L.; Hadt, R. G.; Zheng, S.-L.; Chen, Y.-S.; Nocera, D. G., Trap-Free Halogen Photoelimination from Mononuclear Ni(III) Complexes. *J. Am. Chem. Soc.* **2015,** *137*, 6472-6475.
26. Gonzalez, M. I.; Gygi, D.; Qin, Y.; Zhu, Q.; Johnson, E. J.; Chen, Y.-S.; Nocera, D. G., Taming the Chlorine Radical: Enforcing Steric Control over Chlorine-Radical-Mediated C–H Activation. *J. Am. Chem. Soc.* **2022,** *144*, 1464-1472.
27. Bühler, R. E.; Ebert, M., Transient Charge-transfer Complexes with Chlorine Atoms by Pulse Radiolysis of Carbon Tetrachloride Solutions. *Nature* **1967,** *214*, 1220-1221.
28. Li, G.; Ward, W. M.; Meyer, G. J., Visible Light Driven Nanosecond Bromide Oxidation by a Ru Complex with Subsequent Br–Br Bond Formation. *J. Am. Chem. Soc.* **2015,** *137*, 8321-8323.
29. Li, G.; Swords, W. B.; Meyer, G. J., Bromide Photo-oxidation Sensitized to Visible Light in Consecutive Ion Pairs. *J. Am. Chem. Soc.* **2017,** *139*, 14983-14991.
30. Wehlin, S. A. M.; Troian-Gautier, L.; Li, G.; Meyer, G. J., Chloride Oxidation by Ruthenium Excited-States in Solution. *J. Am. Chem. Soc.* **2017,** *139*, 12903-12906.
31. Li, P.; Deetz, A. M.; Hu, J.; Meyer, G. J.; Hu, K., Chloride Oxidation by One- or Two-Photon Excitation of N-Phenylphenothiazine. *J. Am. Chem. Soc.* **2022,** *144*, 17604-17610.
32. Bevernaegie, R.; Wehlin, S. A. M.; Elias, B.; Troian-Gautier, L., A Roadmap Towards Visible Light Mediated Electron Transfer Chemistry with Iridium(III) Complexes. *ChemPhotoChem* **2021,** *5*, 217-234.
33. Troian-Gautier, L.; Marcelis, L.; De Winter, J.; Gerbaux, P.; Moucheron, C., Two ruthenium complexes capable of storing multiple electrons on a single ligand - photophysical, photochemical and electrochemical properties of [Ru(phen)2(TAPHAT)]2+ and [Ru(phen)2(TAPHAT)Ru(phen)2]4+. *Dalton Trans.* **2017,** *46*, 15287-15300.
34. Bolger, J.; Gourdon, A.; Ishow, E.; Launay, J.-P., Mononuclear and Binuclear Tetrapyrido[3,2-a:2‘,3‘-c:3‘‘,2‘‘-h:2‘‘‘,3‘‘‘-j]phenazine (tpphz) Ruthenium and Osmium Complexes. *Inorg. Chem.* **1996,** *35*, 2937-2944.

35. The fate of the halogen atom formed after excited-state electron transfer is currently not known. Evidence for I2•- formation was obtained at higher concentration of TBAI with additional contributions around 400 nm and 750 nm in the transient absorption spectra. Additional reactions via, for example, hydrogen atom abstraction from the solvent cannot be ruled out at this stage. This could also promote larger cage-escape yields by decreasing the back-electron transfer rate.

36. Gardner, J. M.; Abrahamsson, M.; Farnum, B. H.; Meyer, G. J., Visible Light Generation of Iodine Atoms and I−I Bonds: Sensitized I− Oxidation and I3− Photodissociation. *J. Am. Chem. Soc.* **2009,** *131*, 16206-16214.

37. Note that, at this stage, experiments in neat water were not possible due to the scarce solubility of the iridium dinuclear photosensitizers.

38. Chifotides, H. T.; Schottel, B. L.; Dunbar, K. R., The π-Accepting Arene HAT(CN)6 as a Halide Receptor through Charge Transfer: Multisite Anion Interactions and Self-Assembly in Solution and the Solid State. *Angew. Chem. Int. Ed.* **2010,** *49*, 7202-7207.

39. Ripak, A.; De Kreijger, S.; Elias, B.; Troian-Gautier, L., A protocol for determining cage-escape yields using nanosecond transient absorption spectroscopy. *STAR Protocols* **2023,** *4*, 102312.

40. Aydogan, A.; Bangle, R. E.; Cadranel, A.; Turlington, M. D.; Conroy, D. T.; Cauët, E.; Singleton, M. L.; Meyer, G. J.; Sampaio, R. N.; Elias, B.; Troian-Gautier, L., Accessing Photoredox Transformations with an Iron(III) Photosensitizer and Green Light. *J. Am. Chem. Soc.* **2021,** *143*, 15661-15673.

41. Aydogan, A.; Bangle, R. E.; De Kreijger, S.; Dickenson, J. C.; Singleton, M. L.; Cauët, E.; Cadranel, A.; Meyer, G. J.; Elias, B.; Sampaio, R. N.; Troian-Gautier, L., Mechanistic investigation of a visible light mediated dehalogenation/cyclisation reaction using iron(iii), iridium(iii) and ruthenium(ii) photosensitizers. *Catal. Sci. Technol.* **2021,** *11*, 8037-8051.

42. Ripak, A.; De Kreijger, S.; Sampaio, R. N.; Vincent, C. A.; Cauët, É.; Jabin, I.; Tambar, U. K.; Elias, B.; Troian-Gautier, L., Photosensitized activation of diazonium derivatives for C–B bond formation. *Chem Catal.* **2023**, 100490.

43. Mallouk, T. E.; Krueger, J. S.; Mayer, J. E.; Dymond, C. M. G., Reductive quenching of ruthenium polypyridyl sensitizers by cyanometalate complexes. *Inorg. Chem.* **1989,** *28*, 3507-3510.

44. Yoshimura, A.; Hoffman, M. Z.; Sun, H., An evaluation of the excited state absorption spectrum of Ru(bpy)32+ in aqueous and acetonitrile solutions. *J. Photoch. Photobio. A* **1993,** *70*, 29-33.

45. Goez, M.; von Ramin-Marro, D.; Othman Musa, M. H.; Schiewek, M., Photoionization of [Ru(bpy)3]2+: A Catalytic Cycle with Water as Sacrificial Donor. *J. Phys. Chem. A* **2004,** *108*, 1090-1100.

46. Müller, P.; Brettel, K., [Ru(bpy)3]2+ as a reference in transient absorption spectroscopy: differential absorption coefficients for formation of the long-lived 3MLCT excited state. *Photochem. Photobio. Sci.* **2012,** *11*, 632-636.

47. Farnum, B. H.; Jou, J. J.; Meyer, G. J., Visible light generation of I–I bonds by Ru-tris(diimine) excited states. *Proc. Natl. Acad. Sci. USA* **2012,** *109*, 15628-15633.

48. Farnum, B. H.; Gardner, J. M.; Marton, A.; Narducci-Sarjeant, A. A.; Meyer, G. J., Influence of ion pairing on the oxidation of iodide by MLCT excited states. *Dalton Trans.* **2011,** *40*, 3830-3838.

49. Deetz, A. M.; Meyer, G. J., Resolving Halide Ion Stabilization through Kinetically Competitive Electron Transfers. *JACS Au* **2022,** *2*, 985-995.

50. Deetz, A. M.; Goodwin, M. J.; Kober, E. A.; Meyer, G. J., Nanosecond Intra-Ionic Chloride Photo-Oxidation. *Inorg. Chem.* **2023**.

For TOC use only

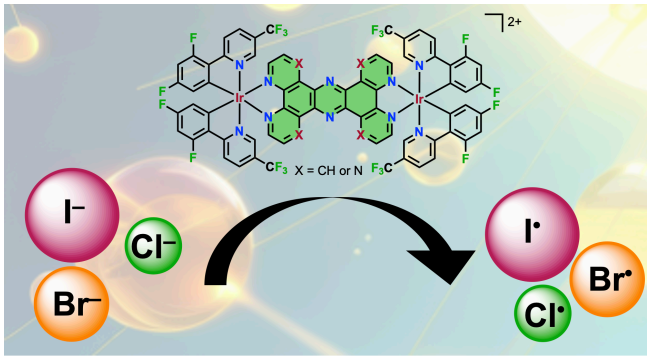

Two novel Ir(III) binuclear photosensitizers are reported for the visible-light induced oxidation of iodide, bromide and chloride in acetonitrile/water mixtures containing up to 50% of water. Excited-state electron transfer was investigated and confirmed by Stern-Volmer quenching experiments and nanosecond transient absorption spectroscopy. Cage-escape yields were quantified by comparative actinometry. These yields were large (96-55%) in acetonitrile and dropped below 32% when 50% of water was present.